

The Ditertiary-Phosphane-Bridged Heteronuclear Cluster $\text{RuOs}_3(\mu\text{-H})_2(\text{CO})_9(\mu\text{-CO})_2(\mu\text{-dppm})$: Synthesis and Reactivity with Alkynes

Yong Leng Kelvin Tan^[a] and Weng Kee Leong^{*[a]}

Keywords: Heterometallic complexes / Ruthenium / Osmium / Ditertiary phosphanes / Alkynes

A high-yielding alternative synthesis of the dppm-bridged heteronuclear cluster $\text{RuOs}_3(\mu\text{-H})_2(\text{CO})_9(\mu\text{-CO})_2(\mu\text{-dppm})$ (**1**) [dppm = bis(diphenylphosphanyl)methane] has been developed. Thermolysis of **1** resulted in dephenylation of both phosphane groups to afford the butterfly cluster $\text{RuOs}_3(\text{CO})_{12}(\mu_4, \kappa^2: \kappa^2\text{-PhPCH}_2\text{PPh})$ (**2**). The reaction of **1** with selected alkynes afforded the products $\text{RuOs}_3(\mu\text{-H})(\text{CO})_8(\mu\text{-CO})(\mu_3, \kappa^2: \kappa^1\text{-PhPCH}_2\text{PPh}_2)(\mu_3, \eta^1: \eta^2: \eta^1\text{-L})$ (**3**) (L = alkyne) in which the alkyne is aligned parallel to an Os–Os bond

(// Os–Os isomer). The clusters incorporating internal alkynes underwent isomerization to the //Ru–Os isomer by alkyne and hydride migration. Several other cluster products of these reactions were also identified, including $\text{RuOs}_3(\mu\text{-H})(\text{CO})_8(\mu\text{-CO})(\mu_3, \kappa^2: \kappa^1\text{-PhPCH}_2\text{PPh}_2)(\mu_3, \eta^1: \eta^2: \eta^1\text{-}t\text{BuC}_2\text{CHO})$ (**6**) in which the methyl group of the alkyne has been oxidized to an aldehyde.

(© Wiley-VCH Verlag GmbH & Co. KGaA, 69451 Weinheim, Germany, 2007)

1. Introduction

Ditertiary phosphane ligands continue to play an important role in the chemistry of transition-metal clusters because they have the ability to maintain the integrity of the metal framework during chemical reactions, preventing cluster fragmentation and enhancing the catalytic activity of the ditertiary-phosphane-stabilized cluster. Several tri- and tetranuclear ruthenium clusters containing ditertiary phosphane ligands have been studied for their catalytic potential in alkene hydrogenation and isomerization reactions.^[1] For these studies, the presence of the phosphane ligand ensured that cluster nuclearity was maintained even under severe reaction conditions. These clusters were found to exhibit greater thermal stability and lower tendency towards decomposition at higher pressure, clearly pointing to the cluster-stabilizing properties of the ditertiary phosphane ligand. In contrast, the catalytic potential of heteronuclear clusters incorporating ditertiary phosphane ligands remains relatively unexplored. The combination of different transition metals within the same framework in heteronuclear clusters may induce novel forms of substrate activation, thus giving rise to interesting chemistry. We have been investigating the chemistry of the hetero group 8 tetranuclear cluster $\text{RuOs}_3(\mu\text{-H})_2(\text{CO})_{13}$ and its derivatives.^[2] In the course of our investigations, we have found that the cluster fragments at elevated temperatures. Our efforts to incorporate the dppm ligand onto the cluster by TMNO (trimethylamine-*N*-oxide) activation have led to the isolation of

$\text{RuOs}_3(\mu\text{-H})_2(\text{CO})_9(\mu\text{-CO})_2(\mu\text{-dppm})$ (**1**) in moderate yield (57%), together with other products.^[3] We were interested in further exploring the reactivity and catalytic potential of **1**. In this paper, we would like to report an alternative, high-yield, synthetic route to **1** and our investigations into its reactions with a number of representative alkynes.

2. Results and Discussion

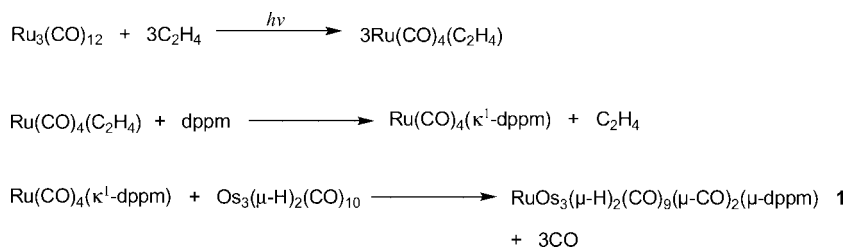
2.1. Synthesis and Thermal Stability of $\text{RuOs}_3(\mu\text{-H})_2(\text{CO})_9(\mu\text{-CO})_2(\mu\text{-dppm})$ (**1**)

The mononuclear ruthenium complex $\text{Ru}(\text{CO})_4(\kappa^1\text{-dppm})$, which can be prepared in situ by treating dppm with $\text{Ru}(\text{CO})_4(\text{C}_2\text{H}_4)$,^[4] has been shown to be a versatile building block for increasing cluster nuclearity. The pendant arm of the ditertiary phosphane can aid the joining of the mononuclear complex to the target cluster; subsequently, metal–metal interactions can be facilitated between the two units held in close proximity to each other.^[5] Thus the addition of $\text{Os}_3(\mu\text{-H})_2(\text{CO})_{10}$ to a hexane solution of $\text{Ru}(\text{CO})_4(\kappa^1\text{-dppm})$ resulted in an instantaneous color change to light yellow. Subsequent workup afforded **1** in 82% yield; the minor side products obtained were $\text{Ru}_3(\text{CO})_{12}$ and $\text{RuOs}_3(\mu\text{-H})_2(\text{CO})_{13}$ (Scheme 1).

Thermolysis of **1** in refluxing hexane afforded the novel butterfly cluster $\text{RuOs}_3(\text{CO})_{12}(\mu_4, \kappa^2: \kappa^2\text{-PhPCH}_2\text{PPh})$ (**2**) and the trinuclear cluster $\text{Os}_3(\mu\text{-H})_2(\text{CO})_8(\mu\text{-dppm})$ in 69% and 15% yields, respectively. The unsaturated, 46-electron hydrido osmium cluster $\text{Os}_3(\mu\text{-H})_2(\text{CO})_8(\mu\text{-dppm})$ has previously been obtained by the treatment of either $\text{Os}_3(\mu\text{-H})(\text{CO})_8[\text{Ph}_2\text{PCH}_2\text{PPh}(\text{C}_6\text{H}_4)]$ or $\text{Os}_3(\mu\text{-H})_2(\text{CO})_7(\mu\text{-dppm})(\mu_3\text{-CN}_2)$ with hydrogen gas at elevated tempera-

[a] Department of Chemistry, National University of Singapore, Kent Ridge, Singapore 119260

Supporting information for this article is available on the WWW under <http://www.eurjic.org> or from the author.



Scheme 1.

tures.^[6] The novel cluster **2** has been completely characterized by spectroscopic, elemental and single-crystal X-ray crystallographic analyses; an ORTEP plot showing the atomic numbering scheme and selected bond parameters are given in Figure 1.

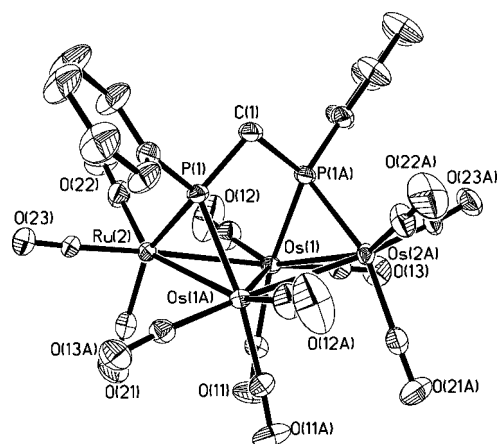


Figure 1. ORTEP diagram (50% probability thermal ellipsoids, organic hydrogen atoms omitted). Selected bond lengths [Å] and angles [°] for **2**: Os(1)–Os(1A) = 2.9067(6), Os(1)–Ru(2) = 2.9289(6), Os(1A)–Ru(2) = 2.8236(6), P(1)–Os(1A) = 2.3591(14), P(1)–Ru(2) = 2.3228(15); Ru(2)–Os(1)–Os(1A) = 61.456(16), Os(1)–Os(1A)–Ru(2) = 57.875(12), Os(1A)–Ru(2)–Os(1) = 60.669(13), Ru(2)–P(1)–Os(1A) = 74.18(4). There is Ru/Os disorder (1:1) over Ru(2) and Os(2A).

The cluster valence electron count for cluster **2** is 62, which is in accord with that predicted by the effective atomic number (EAN) rule for a tetranuclear cluster with five metal–metal bonds.^[7] The dihedral angle between the two wings of the butterfly core of **2** is 150.9°. Dephenylation at each phosphane of the ligand has led to phosphanido bridges across two metal–metal bonds. The phenyl groups were probably lost as benzenes with the cluster-bound hydrides.^[1c,8] There is a total of twelve carbonyl groups on the cluster, compared to eleven in cluster **1**, the additional carbonyl ligand presumably coming from other decomposition products of the reaction.

The spectroscopic data obtained confirms that the solid-state structure of **2** is retained in solution. The $^3\text{1P}\{^1\text{H}\}$ NMR spectrum comprised two sets of doublets at $\delta = 77.40$ and -22.34 ppm. A downfield shift of the phosphorus signals relative to those observed for **1**, in addition to the large $^2J_{\text{PP}}$ of 116.4 Hz, supported the presence of two bridging phosphanido moieties.^[9] On the basis of previous observations that a phosphanido bridge across an Os–Os bond res-

onates at a higher field than one across a Ru–Os edge,^[2b,10] the higher-field phosphorus resonance has been assigned to the phosphanido bridging the Os–Os bond.

2.2. Reaction of **1** with Alkynes

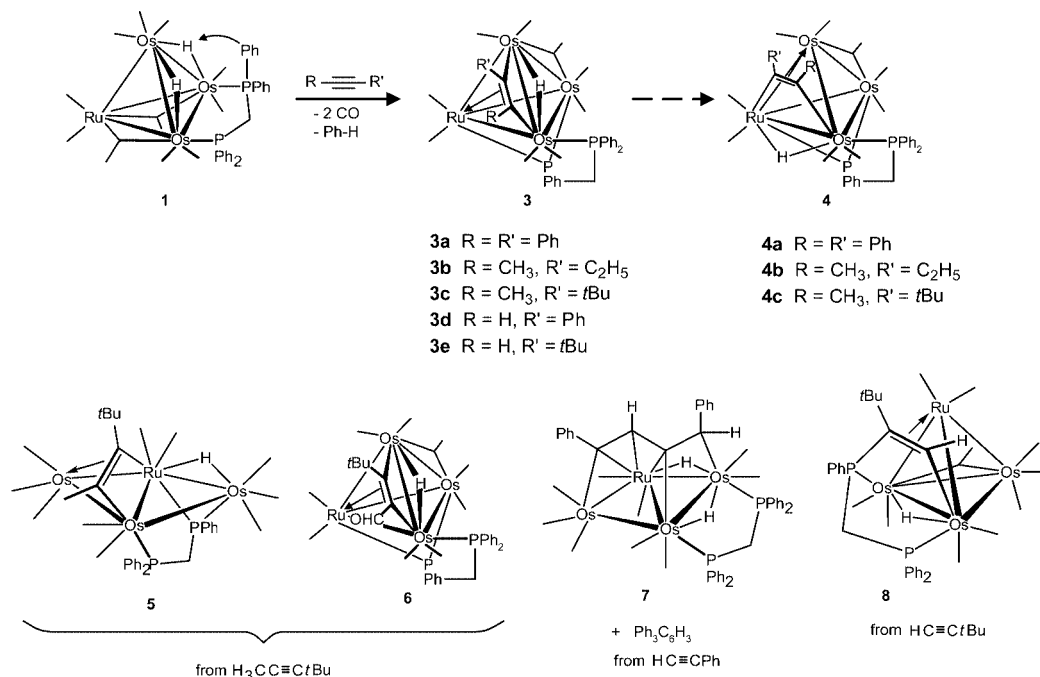
The reaction of **1** with the alkynes diphenylacetylene, 2-pentyne, 4,4-dimethyl-2-pentyne, phenylacetylene, or *tert*-butylacetylene, at elevated temperatures, afforded up to two products, **3** and **4**, each with the general formula $\text{RuOs}_3(\mu\text{-H})(\text{CO})_8(\mu_3\kappa^2\text{-}\kappa^1\text{-PhPCH}_2\text{PPh}_2)(\mu_3\eta^1\text{-}\eta^2\text{-}\eta^1\text{-L})$ [L = PhCCPh (**a**), $\text{C}_2\text{H}_5\text{CCCH}_3$ (**b**), $t\text{BuCCCH}_3$ (**c**) for **3** and **4**; PhCCH (**d**), $t\text{BuCCH}$ (**e**) for **3** (products **4d** and **4e** were not obtained)], as well as some other minor products in some cases (Scheme 2).

Clusters **3** and **4** are isomers differing in whether the $\mu_3\eta^1\text{-}\eta^2\text{-}\eta^1$ -bonded alkyne is parallel to an Os–Os edge (\parallel Os–Os isomer, **3**), or to an Ru–Os edge (\parallel Ru–Os isomer, **4**). Clusters **3** and **4** are also of interest because, in general, tetranuclear clusters tend to form butterfly clusters on reaction with alkynes, i.e., cleavage of a metal–metal bond is common.^[11] Thus there are rarely examples in which the tetrahedral core is retained.^[2g,12] In the formation of these clusters, dephenylation of one of the phosphane groups of the dppm ligand has occurred. Clusters **3** and **4** have been characterized spectroscopically and analytically, and for **3a–e** and **4a–b**, by single-crystal X-ray crystallographic studies as well; the ORTEP plots for **3b** and **4b** are shown in Figure 2 and Figure 3, respectively.

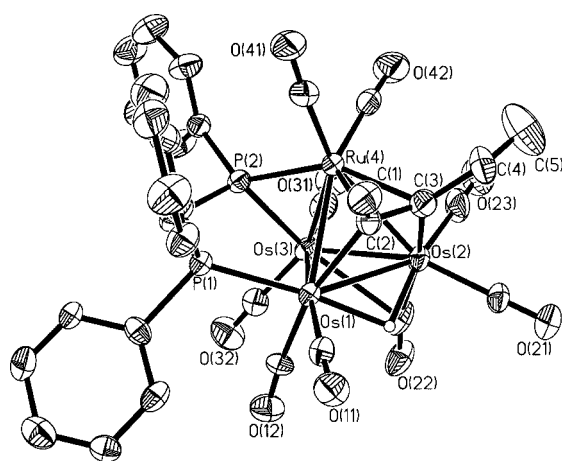
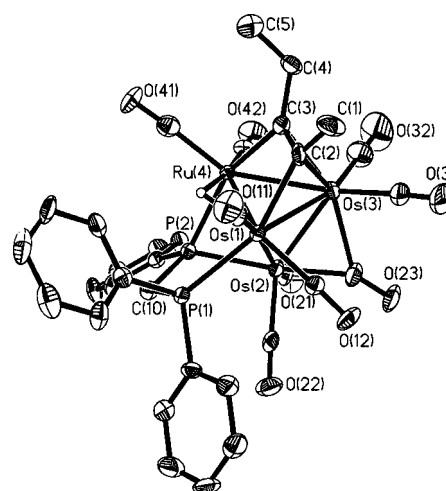
2.3. Structural Discussion on **3** and **4**

Selected bond parameters and a common atomic numbering scheme for clusters **3a–e** are given in Table 1.

The metal core in clusters **3** adopts a closed tetrahedral geometry, with a valence electron count of 60, as predicted by the EAN rule.^[7] The five-electron donor PhPCH₂PPh₂ phosphanido-phosphane ligand caps the Os(1)–Os(2)–Ru(4) triangular metal face of the tetrahedron, the phosphanido group adopting an asymmetrical bridging mode in which the Os(2)–P(2) bond is significantly shorter than the Ru(4)–P(2) bond. C–C bond elongation of the coordinated alkynes is observed, with lengths ranging from 1.366(14) to 1.426(12) Å, which are in the ranges of carbon–carbon sp^2 – sp^2 double and single bonds (1.32 and 1.48 Å, respectively).^[13] In principle, for such unsymmetrical alkynes, there is the possibility of alkyne isomerism, i.e., the forma-



Scheme 2.

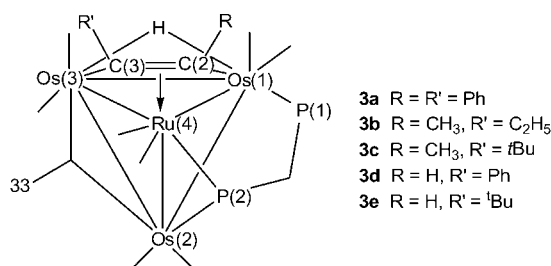
Figure 2. ORTEP diagram (50% probability thermal ellipsoids, organic hydrogen atoms omitted) for **3b**.Figure 3. ORTEP diagram (50% probability thermal ellipsoids, organic hydrogen atoms omitted) for **4b**.

tion of isomers which differ in the orientation of the substituents on the alkyne with respect to the phosphanido bridge.^[14] The stereoselectivity in **3** may be rationalized by the steric interaction between the phosphane ligand and the bulkier substituent on the alkyne moiety.

The metal–metal bond lengths for **3** show some fairly clear trends. The longest metal–metal contact in the tetrahedral core is in the triangular metal face capped by the phosphanido-phosphane moiety; the lengthening of the Os(1)–Os(2) vector is likely to have resulted from the need to accommodate the steric demands imposed by the phosphanido-phosphane ligand. In comparison to the corresponding distances in $\text{RuOs}_3(\mu\text{-PPh}_2)(\mu\text{-H})_3(\text{CO})_{11}$, $\text{RuOs}_3(\mu\text{-PPh}_2)_2$ -

$(\mu\text{-H})_2(\text{CO})_{10}$, $\text{RuOs}_3(\mu\text{-PPh}_2)_2(\mu\text{-H})_4(\text{CO})_9$, and $\text{RuOs}_3(\mu\text{-PPh}_2)(\mu\text{-H})_3(\text{CO})_{10}(\text{PPh}_3)$,^[2b] the phosphanido-bridged Os(2)–Ru(4) bond in **3** (average 2.788 Å) is shorter. One interesting feature is that the Os(1)–Os(3) bond does not display the usual lengthening associated with a hydride-bridged metal–metal vector. This may be ascribed to the presence of the alkyne ligand, which also spans the same edge, therefore countering the normal lengthening effect. The shortest metal–metal separation in the cluster [Os(2)–Os(3)] is associated with the bridging carbonyl group.

A similar tabulation for **4a** and **4b** is given in Table 2; attempts to grow suitable crystals of **4c** proved unsuccessful. There are two crystallographically independent molecules

Table 1. Common atomic numbering scheme and selected bond parameters for clusters **3**.

	3a	3b	3c	3d	3e ^[a]
Bond lengths [Å]					
Os(1)–Os(2)	2.9138(4)	2.9090(5)	2.8837(4)	2.9005(3)	2.8856(11)
Os(1)–Os(3)	2.8564(4)	2.8607(5)	2.8394(4)	2.8607(3)	2.8667(7)
Os(1)–Ru(4)	2.7691(6)	2.7756(8)	2.7760(5)	2.7594(4)	2.7743(7)
Os(2)–Os(3)	2.6662(4)	2.7171(5)	2.7174(4)	2.7028(3)	2.7307(11)
Os(2)–Ru(4)	2.7950(6)	2.7799(8)	2.7713(5)	2.7983(4)	2.7977(11)
Os(3)–Ru(4)	2.8631(6)	2.8060(8)	2.8045(5)	2.8268(4)	2.8237(7)
Os(1)–P(1)	2.3584(18)	2.336(2)	2.3405(17)	2.3406(14)	2.337(3)
Os(2)–P(2)	2.2472(19)	2.242(2)	2.2514(17)	2.2362(14)	2.231(3)
Ru(4)–P(2)	2.3503(18)	2.340(3)	2.3436(17)	2.3210(14)	2.326(3)
Os(2)–C(33)	2.525(8)	2.582(10)	2.575(7)	2.578(6)	2.565(16)
Os(3)–C(33)	2.004(9)	1.960(13)	1.981(7)	1.955(7)	1.948(16)
Os(1)–C(2)	2.191(7)	2.138(10)	2.168(6)	2.141(5)	2.117(13)
Os(3)–C(3)	2.080(8)	2.133(10)	2.159(6)	2.102(5)	2.12(13)
C(2)–C(3)	1.423(10)	1.386(14)	1.409(9)	1.401(7)	1.397(18)
Bond angles [°]					
Os(2)–P(2)–Ru(4)	74.84(6)	74.68(7)	74.15(5)	75.74(4)	75.71(10)
Os(2)–C(33)–Os(3)	71.1(3)	72.0(3)	71.9(2)	71.7(2)	73.0(5)

[a] Disorder of ruthenium over Os(2) and Ru(4).

in the asymmetric unit of **4a**; their bond parameters are fairly similar. The crystals of both **4a** and **4b** exhibited disorder of the ruthenium atom about two alternative sites in the metal framework. This disorder was solved with ruthenium occupancies of about 0.08 and 0.92 at M(3) and M(4), respectively, for **4a**, and 0.07 and 0.93 at M(3) and M(4), respectively, for **4b**. As in **3**, the phosphanido-phosphane bridged Os(1)–Os(2) edge is the longest metal–metal bond in the tetrahedral core, while the carbonyl-bridged Os(2)–Os(3) bond is the shortest.

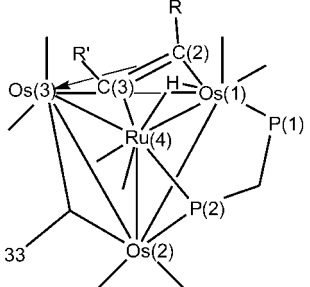
The NMR spectra of both **4a** and **4b** indicated the presence of two isomers in an approximately 11:1 ratio in solution. The hydride resonances for each of these isomers appear as doublets of doublets of doublets; the coupling constants have been confirmed by selective decoupling experiments. The splitting pattern and values of the coupling constants provided further evidence that the hydride bridges the same metal–metal edge as the phosphanido-phosphane ligand and is found in a *cisoid* position relative to the two phosphorus atoms. Both the ³¹P{¹H} and the ¹H NMR spectra of **4c** indicated that three isomers are present in an approximately 8:1:1 ratio in solution. ³¹P{¹H}–³¹P{¹H} COSY and ³¹P{¹H}–¹H HMBC experiments were carried out to aid the elucidation of the P–P and P–H correlations, while the coupling constants were confirmed by ¹H{³¹P}

selective decoupling experiments. A 2D ¹H EXSY experiment performed at ambient temperature indicated no chemical exchange between the three isomers of **4c**. The proposed solution-state structures and tentative NMR assignments for **4a–c** are shown in Figure 4, and at least for **4a** and **4b**, are consistent with the disorder observed in the solid state.^[2c–2f]

The hydride resonances for **4** were shifted upfield relative to those for the corresponding isomer **3**. This may be ascribed to an increase in electron density at the hydride for **4**, since the hydride spans the Os(1)–Ru(4) edge, which contains the bridging phosphanido-phosphane ligand and is thus expected to be the most electron-rich metal–metal bond.^[15] The two phosphorus resonances for **4a–c** are also shifted downfield relative to **3a–c**. More notably, the values of the ²J_{PP} coupling constants for **4a–c** are almost twice those found for **3a–c**, although the P–C–P bond angle in the two isomers do not differ significantly.

2.4. Isomerism of **3a–c** to **4a–c**

Thermolysis of **3a–c** afforded the isomeric products **4a–c**, respectively; clusters **3d** and **3e** (which incorporated terminal alkynes) did not exhibit isomerization under similar

Table 2. Common atomic numbering scheme and selected bond parameters for **4a** and **4b**.


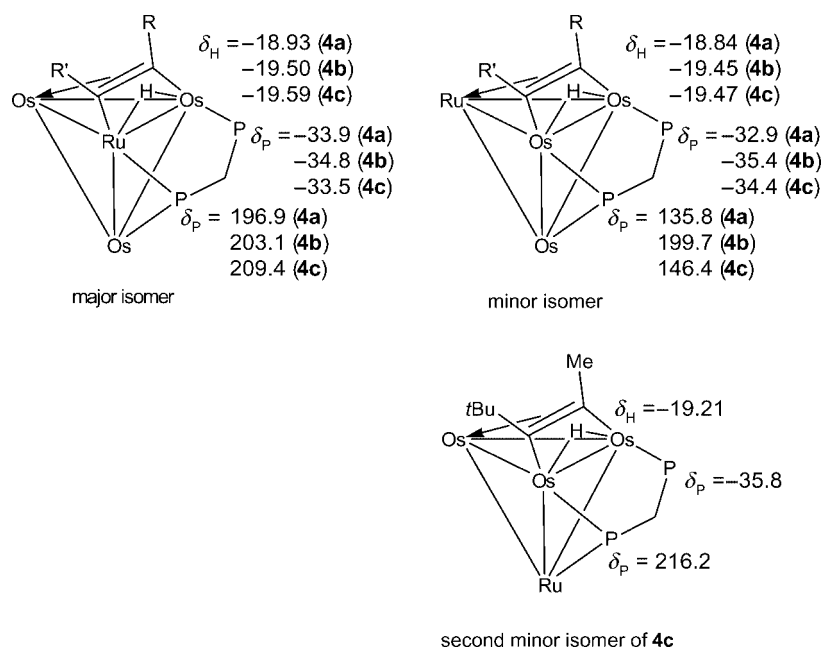
4a R = R' = Ph
4b R = CH₃, R' = C₂H₅

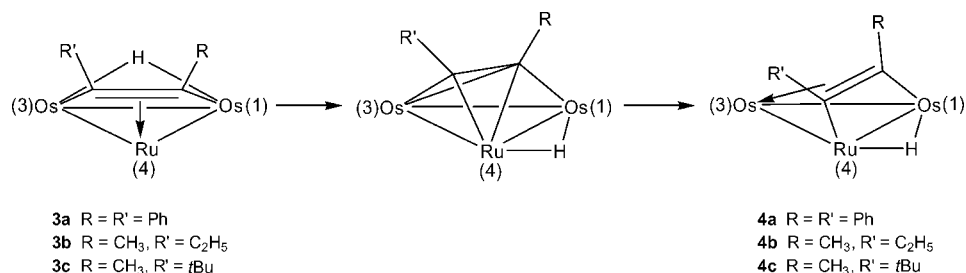
	4a (Molecule A) ^[a]	4a (Molecule B) ^[a]	4b ^[b]
Bond lengths [Å]			
Os(1)–Os(2)	2.9210(14)	2.9184(14)	2.9272(5)
Os(1)–Os(3)	2.7774(15)	2.7730(15)	2.7744(5)
Os(1)–Ru(4)	2.837(2)	2.843(2)	2.8360(7)
Os(2)–Os(3)	2.6114(15)	2.6290(16)	2.6281(5)
Os(2)–Ru(4)	2.821(2)	2.807(2)	2.7955(7)
Os(3)–Ru(4)	2.786(2)	2.777(2)	2.7682(7)
Os(1)–P(1)	2.384(7)	2.377(7)	2.376(2)
Os(2)–P(2)	2.338(7)	2.331(7)	2.335(2)
Ru(4)–P(2)	2.327(7)	2.325(7)	2.341(9)
Os(2)–C(33)	1.96(3)	2.00(3)	2.039(9)
Os(3)–C(33)	2.39(3)	2.36(3)	2.287(9)
Os(1)–C(2)	2.18(2)	2.21(2)	2.134(9)
Ru(4)–C(3)	2.13(3)	2.15(3)	2.111(8)
C(2)–C(3)	1.42(3)	1.42(3)	1.411(12)
Bond angles [°]			
Os(2)–P(2)–Ru(4)	74.4(2)	74.2(2)	73.42(6)
Os(2)–C(33)–Os(3)	73.1(10)	73.6(9)	74.6(3)

[a] Disorder of Ru over Os(3) and Ru(4), with Ru occupancies of 8 and 92%, respectively. [b] Disorder of Ru over Os(3) and Ru(4), with Ru occupancies of 7 and 93%, respectively.

conditions. Clusters **3** and **4** are the kinetic and thermodynamic products, respectively. It has been noticed that, in several heterometallic clusters, the coordinated alkynes are apparently oriented such that the π -bond is directed towards the less electron-rich metal.^[16] Likewise, in ditertiary-phosphane-substituted trisodium clusters incorporating hydride ligands, the hydride is observed to occupy the most electron-rich metal–metal bond in the cluster.^[15] In **4**, the Os(1) and Ru(4) metal atoms are electron-rich as a result of σ -donation from the ligating phosphanido-phosphane moiety, which probably is the driving force for the reorientation of the alkyne and hydride over the Os(1)–Os(3)–Ru(4) edge.

The isomerization of **3a–c** to **4a–c** involves a flipping of the alkyne ligand about the Os(1)–Os(3)–Ru(4) face, coupled with hydride migration from the Os(1)–Os(3) to the Os(1)–Ru(4) edge. It is envisaged that this dynamic process occurs via an intermediate in which the alkyne is coordinated in a $\mu_3, \eta^2: \eta^2$ perpendicular fashion (Scheme 3). Such a process has been previously proposed to account for the observed rotation of parallel-coordinated alkynes on a trisodium cluster.^[17] More recently, a reversed scheme termed *switchback motion* has been suggested to explain the fluxional behavior of the triruthenium cluster $[\{\text{Cp}^*\text{Ru}(\mu\text{-H})_3(\mu_3, \eta^2: \eta^2\text{-C}_5\text{H}_6)\}]$.^[18] We have monitored the isomerization of **3c** to **4c** by ¹H NMR spectroscopy and found that it is a very slow process at ambient temperature. After five months at ambient temperature, the mixture was heated in refluxing hexane for 4 h in order to obtain the equilibrium concentrations. The final spectrum recorded after thermolysis of the mixture gave $K_{\text{eqm}} = [\mathbf{4c}]_{\text{eqm}}/[\mathbf{3c}]_{\text{eqm}} = 10.9$ and $\Delta G = -RT \ln K_{\text{eqm}} = -5.92 \text{ kJ mol}^{-1}$. The half-life for the isomerization was estimated to be ca. 77 d.

Figure 4. Proposed solution-state structures and tentative NMR assignments for **4** (carbonyl and phenyl groups omitted).



Scheme 3.

2.5. Other Products

A number of other novel clusters were also isolated from these reactions with alkynes, viz. RuOs₃(μ-H)(CO)₁₀(μ₃,κ²:κ¹-PhPCH₂PPh₂)(μ₃,η¹:η²:η¹-*t*BuC₂CH₃) (**5**) and RuOs₃(μ-H)(CO)₈(μ-CO)(μ₃,κ²:κ¹-PhPCH₂PPh₂)(μ₃,η¹:η²:η¹-*t*BuC₂CHO) (**6**) from 4,4-dimethyl-2-pentyne, RuOs₃(μ-H)₂(CO)₉(μ-Ph₂PCH₂PPh₂)(μ₄,η¹:η²:η²:η¹-PhCCHCCHPh) (**7**) from phenylacetylene, and RuOs₃(μ-H)(CO)₉(μ-CO)[μ₃,η¹:η²:κ¹:κ¹-(HC=C*t*Bu)PhPCH₂PPh₂] (**8**) from *tert*-butylacetylene. The characterization of all these clusters is complete, including single-crystal X-ray diffraction studies. The ORTEP plots and selected bond parameters for **5–8** are given in Figure 5, Figure 6, Figure 7, and Figure 8.

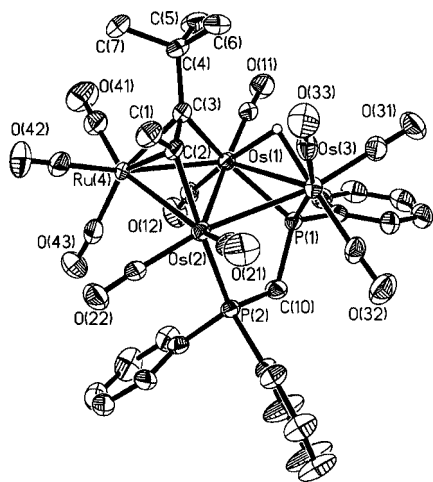


Figure 5. ORTEP diagram (50% probability thermal ellipsoids, organic hydrogen atoms omitted). Selected bond lengths [Å] and angles [°] for **5**: Os(1)–Os(2) = 2.7947(4), Os(1)–Os(3) = 2.8787(4), Os(1)–Ru(4) = 2.7535(5), Os(2)–Os(3) = 2.9403(4), Os(2)–Ru(4) = 2.7854(4), Os(1)–P(1) = 2.3010(16), Os(3)–P(1) = 2.3364(17), Os(2)–P(2) = 2.3965(17), Os(1)–C(3) = 2.204(7), Os(2)–C(2) = 2.089(6), Ru(4)–C(2) = 2.262(7), Ru(4)–C(3) = 2.181(7); Os(1)–P(1)–Os(3) = 76.74(4).

The molecular structure of **5** shows disorder of the heavy atoms, which was solved with ruthenium occupancies of 0.33 and 0.67 at M(1) and M(4), respectively. Cluster **5** comprises an open butterfly-shaped tetranuclear metal core, the two wings of the butterfly cluster having a dihedral angle of 157.6° between them. A metal-bound hydride bridges the Os(1)–Os(3) vector. The position of this hydride was located by a low-angle difference map and verified by XHYDEX calculations.^[19] One triangular wing of the but-

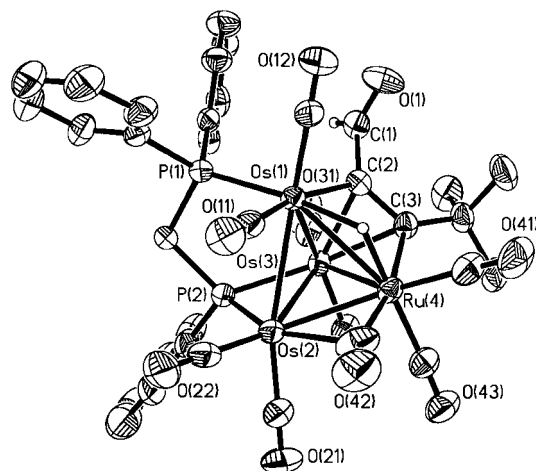


Figure 6. ORTEP diagram (50% probability thermal ellipsoids, organic hydrogen atoms omitted). Selected bond lengths [Å] and angles [°] for **6**: Os(1)–Os(2) = 2.9020(4), Os(1)–Os(3) = 2.7885(5), Os(1)–Ru(4) = 2.8649(5), Os(2)–Os(3) = 2.7861(5), Os(2)–Ru(4) = 2.7061(5), Os(3)–Ru(4) = 2.8001(5), Os(1)–P(1) = 2.3516(18), Os(2)–P(2) = 2.252(2), Os(3)–P(2) = 2.321(2), Os(1)–C(2) = 2.164(7), Os(3)–C(2) = 2.156(7), Os(3)–C(3) = 2.235(7), Ru(4)–C(3) = 2.135(7); Os(2)–P(2)–Os(3) = 75.05(6), Ru(4)–C(42)–Os(2) = 74.1(3).

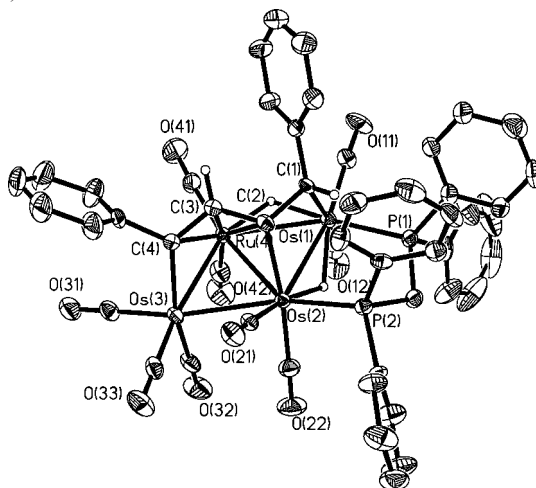


Figure 7. ORTEP diagram (50% probability thermal ellipsoids, organic hydrogen atoms omitted). Selected bond lengths [Å] and angles [°] for **7**: Os(1)–Os(2) = 3.0121(4), Os(1)–Ru(4) = 2.9363(6), Os(2)–Os(3) = 2.9305(4), Os(2)–Ru(4) = 2.8499(6), Os(3)–Ru(4) = 2.6858(6), Os(1)–P(1) = 2.3303(18), Os(2)–P(2) = 2.3546(18), Os(1)–C(1) = 2.240(7), Os(2)–C(2) = 2.098(7), Os(3)–C(4) = 2.081(7), Ru(4)–C(2) = 2.301(7), Ru(4)–C(3) = 2.239(7), Ru(4)–C(4) = 2.249(7), C(1)–C(2) = 1.464(9), C(2)–C(3) = 1.425(10), C(3)–C(4) = 1.434(9); P(1)–Os(1)–Os(2) = 93.90(4), P(2)–Os(2)–Os(1) = 86.17(4).

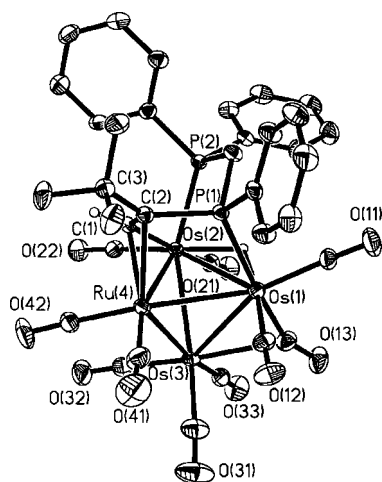


Figure 8. ORTEP diagram (50% probability thermal ellipsoids, organic hydrogen atoms omitted). Selected bond lengths [Å] and angles [°] for **8**: Os(1)–Os(2) = 2.9290(2), Os(1)–Os(3) = 2.8684(2), Os(1)–Ru(4) = 2.8484(3), Os(2)–Os(3) = 2.8319(2), Os(2)–Ru(4) = 2.7656(3), Os(3)–Ru(4) = 2.6588(3), Os(1)–P(1) = 2.3726(10), Os(2)–P(2) = 2.3382(10), Os(2)–C(1) = 2.149(4), P(1)–C(2) = 1.805(4), C(1)–C(2) = 1.407(5), Os(1)–C(13) = 1.984(5), Os(3)–C(13) = 2.478(5); Os(1)–C(13)–Os(3) = 79.16(16).

terfly cluster is capped by the dephenylated dppm ligand, while the other wing is capped by the alkyne moiety, and these ligands are orientated on opposite sides of the plane defined by the four metal atoms.

The $^{31}\text{P}\{^1\text{H}\}$ and ^1H NMR spectra of **5** showed that there were two isomers in solution. The NMR resonances have been assigned with the aid of $^1\text{H}\{^{31}\text{P}\}$ selective decoupling and $^{31}\text{P}\{^1\text{H}\}$ – ^1H HMBC experimental data, and also on the basis of earlier observations that ^{31}P chemical shifts for a phosphanido bridges across Ru–Os edges are found downfield relative to those across Os–Os bonds.^[2b,10] The proposed solution-state structures and their tentative NMR assignments are displayed in Figure 9, and are in agreement with the disorder in the solid-state structure. Thermolysis of **5** afforded **3c** and **4c** in 49% and 46% yields (with respect to the amount of **5** that reacted), respectively, indicating that **5** may be a precursor to **3c**. The formation of **3c** from **5** should be a multistep process, involving the elimination of one CO ligand, migration of hydride and CO ligands, metal–carbon bond cleavage and formation, and metal–metal bond formation, but the sequence of these processes remains unknown.

The crystal of **6** also exhibited disorder of the metal framework, which was solved with ruthenium occupancies of about 0.42 and 0.58 at M(3) and M(4), respectively. Cluster **6** is structurally very similar to **3c**, and it contains almost the same ligand set. The main structural difference is the replacement of the methyl substituent on the coordinated alkyne moiety by an aldehyde functional group. Both the ^1H and $^{31}\text{P}\{^1\text{H}\}$ NMR spectra of **6** displayed two sets of signals integrating to give a 7:1 ratio, indicating the presence of two isomers in solution. The proposed solution-state structures for the two isomers of **6**, which are in agreement with the disorder observed in the solid-state crystal

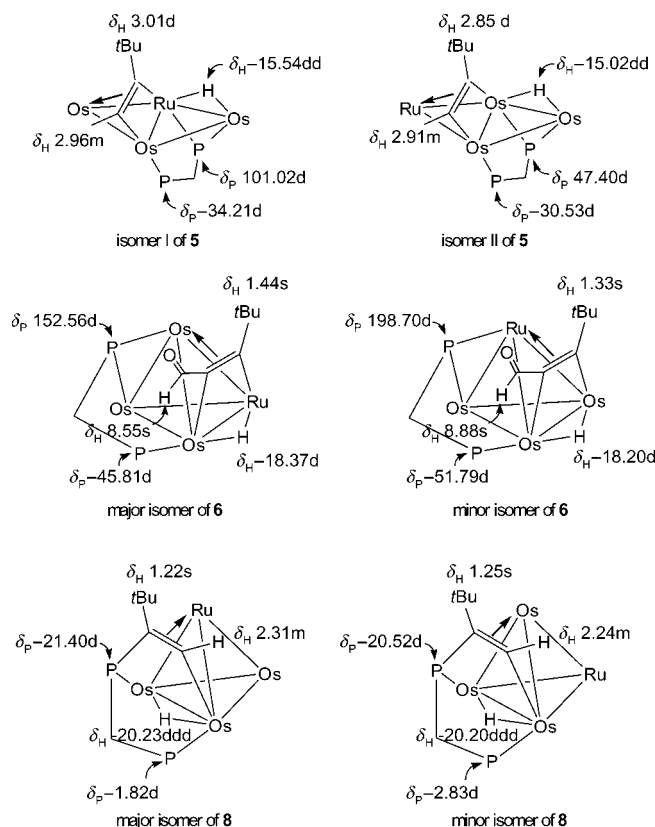


Figure 9. Proposed solution-state structures and tentative NMR assignments for **5**, **6**, and **8** (carbonyl and phenyl groups omitted).

structure, are shown in Figure 9 together with the tentative NMR assignments.

We have carried out a number of experiments to understand how the aldehyde group in **6** could have been formed. Monitoring the reaction of **1** with 4,4-dimethyl-2-pentyne in degassed $[\text{D}_{12}]\text{cyclohexane}$ by ^1H NMR spectroscopy indicated that formation of the aldehyde occurred during the reaction. Carrying out the reaction in the presence of air resulted in a slightly higher yield of **6** (15% vs. 12% in the degassed sample). Cluster **6** was formed even when the reaction was carried out under anhydrous conditions; similarly, the yield of **6** did not increase upon addition of water to the system. Thermolysis of **3c**, **4c**, or **5** in air did not result in the formation of **6**. Oxidation of the methyl group to form the aldehyde prior to alkyne coordination to the metal cluster is unlikely, as previously reported reactions between clusters and unsaturated aldehydes or ketones gave products in which the oxygen atom of the organic carbonyl ligand is coordinated to the metal core.^[20] Presumably the alkyne is oxidized in the presence of **1** to afford **6**, while **3c**, **4c**, and **5** appear not to be involved in this process, although the oxidant remains unknown.

Cluster **7** is another butterfly-shaped tetranuclear cluster, with a dihedral angle of 166.4° between the wing planes. The Os(1)–Os(2) edge is bridged by the dppm ligand, and the metal–phosphorus bond lengths do not differ significantly from those found for the parent cluster **1**. The XHYDEX program indicated that hydride ligands bridged

both Os(1)–Os(2) and Os(1)–Ru(4); this is supported by the observation that these vectors are long [3.0121(4) and 2.9363(6) Å, respectively]. In **7**, two phenylacetylenes have coupled head-to-head, and the resulting four-carbon ligand is coordinated to all four metal atoms, with an η^3 -allylic interaction to Ru(4);^[21] there is no evidence of another isomer displaying head-to-tail coupling, although both types of products have been reported for ruthenium and osmium clusters.^[22] The organic moiety formally donates six electrons, resulting in a cluster electron count of 62 for **7**, in accordance with the effective atomic number (EAN) rule.^[7] Carbon–carbon bond lengths within the organic ligand range from 1.425(10) to 1.464(9) Å, which are in the ranges of carbon–carbon sp^2 – sp^2 double and single bonds (1.32 and 1.48 Å, respectively),^[13] suggesting some electron delocalization over the entire carbon chain. Dimerization of the two alkyne units also resulted in a hydrogen atom shift, which has been postulated to precede the C–C coupling step.^[23] The spectroscopic data for **7** clearly points to the retention of the solid-state structure in solution.

Cluster **8** retains the tetrahedral metal framework of the parent cluster **1**; the long Os(1)–Os(2) edge [2.9290(2) Å] is bridged by both a hydride and a dephenylated dpmm moiety. A salient structural feature in **8** is the formation of a phosphorus–carbon bond between the dephenylated phosphane P(1) and the C(2) carbon of the vinyl organic fragment [P(1)–C(2) = 1.805(4) Å], resulting in the capping of the Os(1)–Os(2)–Ru(4) triangular face of the metal tetrahedron by the novel ligand (HC=C*t*Bu)PhPCH₂PPh₂ in a $\mu_3, \eta^1: \eta^2: \kappa^1: \kappa^1$ manner. Reports of P–C coupling between two separate ligands are rare in cluster chemistry, few examples are known.^[24] This ligand donates a total of seven electrons to the cluster, and **8** is formally a 60-electron species in accordance with the observed tetrahedral metal core. The crystal of **8** also exhibited disorder of the metal framework, which was solved with ruthenium occupancies of about 0.11 and 0.89 at M(3) and M(4), respectively.

The NMR spectra of **8** showed that there are two isomers present in an approximate 9:1 ratio in solution. $^1\text{H}\{^{31}\text{P}\}$ as well as $^1\text{H}\{^1\text{H}\}$ selective decoupling experiments have been utilized to aid the assignment of the signals. The proposed solution-state structures for the isomers of **8** and their tentative NMR assignments are given in Figure 9; the structures, as well as their relative proportions, are in agreement with those expected from the disorder found in the solid state. On prolonged standing in solution, **8** was found to slowly convert to **3e**; this process could be speeded up by thermolysis. Thus, **8** is a precursor to **3e**, but this conversion has to be a multistep process.

In addition to **3d** and **7**, the reaction with phenylacetylene afforded, as characterized by mass spectrometry and ^1H NMR spectroscopy, a mixture of 1,3,5- and 1,2,4-triphenylbenzene.^[25] Gas chromatography-mass spectrometry (GC-MS) analysis indicated that these cyclotrimerized products were present in a 1:2 ratio. We have found that **3d** catalyzed the cyclotrimerization of phenylacetylene; the cluster was recoverable quantitatively and no intermediates could be isolated. A number of organometallic compounds

are known to catalyze the [2+2+2]-cyclotrimerization of alkynes,^[26] but few cluster catalysts are known.^[27] Thus far, attempts at optimization showed that **3d** is at best a modest catalyst, with TON < 2 for a catalyst loading of 1 mol-%. In contrast, **7** failed to react with phenylacetylene under similar conditions, suggesting that it is not directly involved in the catalytic step. Furthermore, **7** was not obtained in the reaction of **3d** with phenylacetylene, indicating that it is not a side product of the catalytic reaction. No cyclotrimerization product was obtained from the reaction of **2** with the other alkynes reported here, and **3d** also failed to catalyze the cyclotrimerization of diphenylacetylene (an internal alkyne) or *tert*-butylacetylene (a terminal alkyne).

3. Concluding Remarks

In this study, we have found that **1** reacts with both terminal and internal alkynes to afford initially cluster **3** in which the alkyne is bonded in a $\mu_3, \eta^1: \eta^2: \eta^1$ fashion and the alkyne C≡C bond is parallel to an Os–Os edge; the tetrahedral core of the cluster is retained. The binding of the alkyne appears to be highly stereoselective, since for unsymmetrical alkynes, the bulkier substituent is oriented away from the dephenylated dpmm moiety. In the case of internal alkynes, **3** isomerized slowly to form **4**. This isomerization process involved migration of both the alkyne and hydride across a triangular metal face to bridge the most electron-rich metal–metal bond of the cluster, which is that bridged by the dephenylated dpmm; the stereoselectivity appears to be similar to that in **3**. Cluster **3d** was also found to be a modest catalyst for the cyclotrimerization of phenylacetylene.

These results point to stereoselective binding of alkynes in such heterometallic clusters, and indicate that the ditertiary phosphane ligand can play an important role in the high stereoselectivity exhibited as well as in keeping the cluster framework intact. Hence, such clusters may play a useful role in the stereocontrol of reactions with alkynes and provide a possible direction for future work.

4. Experimental Section

4.1. General Procedures: All reactions and manipulations were carried out under nitrogen by using standard Schlenk techniques. Solvents were purified, dried, distilled, and stored under nitrogen prior to use. The products were separated by thin layer chromatography (TLC), by using plates coated with silica gel 60 F254 of 0.25 or 0.5 mm thickness and extracted with dichloromethane. Routine NMR spectra were acquired with a Bruker ACF300 NMR spectrometer, while decoupling and 2D NMR spectra were obtained with a Bruker Avance DRX500 or Bruker AMX500 machine. The solvent used was deuterated chloroform unless otherwise stated. Chemical shifts reported are referenced to that for the residual proton of the solvent for ^1H , and to 85% aqueous H_3PO_4 (external standard) for $^{31}\text{P}\{^1\text{H}\}$. Mass spectra were obtained with a Finnigan MAT95XL-T spectrometer in an *m*-nitrobenzyl alcohol matrix. Microanalyses were carried out by the microanalytical laboratory at the National University of Singapore. GC-MS analysis was car-

ried out with an Agilent GC 6890 with Mass Selective Detector MS 5973, using a 300 mm × 0.25 mm × 0.25 μm HP-1 MS column. The cluster Os₃(μ-H)₂(CO)₁₀ was prepared according to the literature method.^[28] Ru₃(CO)₁₂ was purchased from Oxxem Ltd; all other reagents were from commercial sources and were used as supplied.

4.2. Synthesis of RuOs₃(μ-H)₂(CO)₉(μ-CO)₂(μ-dppm) (1): Ru₃(CO)₁₂ (8.0 mg, 0.013 mmol) was placed with hexane (20 mL) into a 100-mL round-bottomed flask fitted with a Teflon valve. After three freeze-pump-thaw cycles, ethene gas at ca. 20 psi was introduced at ambient temperature. The mixture was then irradiated with a 60W Phillips reflector lamp, while being cooled in an ice-water bath, until the solution became colorless (ca. 2 h). Ru(CO)₄(C₂H₄) was formed in quantitative yield, as characterized by infrared spectroscopy. A stoichiometric equivalent of dppm was added to the solution which was still kept in the ice-water bath. Formation of Ru(CO)₄(κ¹-dppm) was established by its infrared spectroscopic data. Addition of Os₃(μ-H)₂(CO)₁₀ (30.1 mg, 0.036 mmol) resulted in an immediate color change to light yellow. The mixture was stirred under a nitrogen atmosphere for 1.5 h. Removal of the solvent and volatiles in vacuo and column chromatographic separation of the residue, with hexane and dichloromethane as eluents, yielded three bands. [Yields are calculated with respect to Os₃(μ-H)₂(CO)₁₀ used.] The first two bands were identified from their infrared spectra as Ru₃(CO)₁₂ (1.2 mg, 0.002 mmol) and RuOs₃(μ-H)₂(CO)₁₃ (5.6 mg, 15%), respectively. The third band was identified from its infrared spectrum as RuOs₃(μ-H)₂(CO)₉(μ-CO)₂(μ-dppm) (**1**) (40.3 mg, 82%).

4.3. Thermolysis of 1: To a Schlenk tube containing **1** (16.9 mg, 0.012 mmol) was added hexane (30 mL), and the reaction mixture was stirred and heated under reflux for 4 h. The solvent was removed under reduced pressure, and the residue obtained was redissolved in a minimum of dichloromethane and chromatographed on TLC plates. Elution with hexane/dichloromethane (4:1, v/v) yielded two bands. Band 1 (*R*_f = 0.49) gave dark red crystals of RuOs₃(CO)₁₂(μ₄,κ²:κ²-PhPCH₂PPh) (**2**). Yield: 10.4 mg, 69%. Band 2 (*R*_f = 0.19) gave dark red crystals of Os₃(μ-H)₂(CO)₈(μ-dppm). Yield: 2.1 mg, 15%. IR (CH₂Cl₂) ν(CO) : $\tilde{\nu}$ = 2068 (s), 2005 (vs), 1983 (vs, br), 1955 (w), 1943 (w) cm⁻¹. ³¹P{¹H} NMR: δ = -0.02 (s) ppm. ¹H NMR: δ = 7.35 (m, 20 H, Ph), 4.19 (t, ²*J*_{PH} = 10.5 Hz, 2 H, CH₂), -10.26 (t, ²*J*_{PH} = 9.9 Hz, 2 H, OsHOs) ppm. MS (FAB): *m/z* calcd. for [M]⁺ 1181; found 1181. X-ray data: Orthorhombic, *Pbca*, *a* = 16.2438(4) Å, *b* = 16.8441(5) Å, *c* = 25.3499(7) Å, *V* = 6936.0(3) Å³. Data are in agreement with literature values.^[6a]

4.4. Reactions of 1 with Alkynes: In a typical reaction, to a Schlenk tube containing **1** and hexane (30 mL) was added the alkyne, and the reaction mixture was stirred and heated under reflux for 6 h. The solvent was removed under reduced pressure, and the residue obtained was redissolved in a minimum of dichloromethane and chromatographed on TLC plates with hexane/dichloromethane (3:2, v/v) as the mobile phase. The reaction conditions and yields are summarized in Table 3, and spectroscopic and analytical data for all new products are given in Table 4 and Table 5.

4.5. Thermolysis of 3: In a typical reaction, to a Schlenk tube containing **3a** (20.2 mg, 14 μmol) was added hexane (30 mL), and the

Table 3. Reaction of **1** with alkynes.

Amount of 1	Alkyne (amount)	Product	Color	<i>R</i> _f	Yield
20.1 mg, 0.014 mmol	PhCCPh (8.0 mg, 0.045 mmol)	3a	dark brown	0.27	19.2 mg, 95%
22.4 mg, 0.016 mmol	C ₂ H ₅ CCCH ₃ (0.1 mL)	4b	red-orange	0.57	8.1 mg, 39%
		3b	red-orange	0.51	7.9 mg, 38%
20.2 mg, 0.014 mmol	<i>t</i> BuCCCH ₃ (0.1 mL)	5	dark brown	0.43	3.1 mg, 17%
		4c	dark brown	0.31	4.7 mg, 25%
		3c	dark brown	0.26	5.7 mg, 30%
		6	dark brown	0.19	2.1 mg, 12%
20.6 mg, 0.014 mmol	PhCCH (0.1 mL)	triphenylbenzene	yellow	0.69	2.1 mg
		3d	dark brown	0.54	8.2 mg, 44%
		7	dark brown	0.40	8.2 mg, 39%
25.8 mg, 0.018 mmol	<i>t</i> BuCCCH (0.1 mL)	3e	dark brown	0.57	12.8 mg, 55%
		8	dark brown	0.37	10.2 mg, 40%

Table 4. Infrared and analytical data for all new products.

Cluster	IR (CH ₂ Cl ₂) ν(CO) [cm ⁻¹]	Elemental analysis: found (calculated) [%]
2	2090 m, 2061 vs, 2030 s, 1997 w (br), 1985 mw	C ₂₅ H ₁₂ O ₁₂ Os ₃ P ₂ Ru·1/4C ₆ H ₁₄ : C, 25.35 (25.27); H, 1.00 (1.24) ^[a]
3a	2065 s, 2018 s, 2005 vs, 1998 vs, 1984 s, 1960 m, 1921 w	C ₄₂ H ₂₈ O ₉ Os ₃ P ₂ Ru·1/2CH ₂ Cl ₂ : C, 34.99 (35.13); H, 1.95 (2.01) ^[b]
3b	2062 s, 2016 s, 2000 vs, 1995 vs, 1979 s, 1956 m, 1931 w, 1915 w	—
3c	2059 s, 2014 s, 2000 vs, 1994 vs, 1979 s, 1959 m, 1915 w	C ₃₅ H ₃₀ O ₉ Os ₃ P ₂ Ru: C, 31.85 (31.61); H, 2.39 (2.25)
3d	2065 s, 2042 w, 2022 s, 2005 vs (br), 1984 s, 1918 w	C ₃₆ H ₂₄ O ₉ Os ₃ P ₂ Ru: C, 33.27 (33.28); H, 2.08 (1.79)
3e	2060 s, 2018 s, 2004 vs, 1996 vs, 1984 s, 1966 m, 1935 w (br)	C ₃₄ H ₂₈ O ₉ Os ₃ P ₂ Ru: C, 31.35 (31.07); H, 1.90 (2.15)
4a	2052 w, 2022 s, 2004 m, 1983 w, 1968 w, 1950 vw (sh)	—
4b	2061 w, 2050 m, 2016 s, 2001 s, 1979 m, 1964 m	C ₃₃ H ₂₆ O ₉ Os ₃ P ₂ Ru·1/2C ₆ H ₁₄ : C, 32.41 (32.19); H, 2.41 (2.48) ^[a]
4c	2058 w, 2049 w, 2015 vs, 2000 s, 1979 m, 1963 m	C ₃₅ H ₃₀ O ₉ Os ₃ P ₂ Ru: C, 31.39 (31.61); H, 2.00 (2.25)
5	2078 w (sh), 2064 vs, 2052 w (sh), 2017 m (sh), 1997 s, 1954 w, 1919 vw	C ₃₆ H ₃₀ O ₁₀ Os ₃ P ₂ Ru: C, 32.28 (31.88); H, 2.02 (2.23)
6	2064 w, 2012 s, 2002 ms, 1989 m, 1966 w	C ₃₅ H ₂₈ O ₁₀ Os ₃ P ₂ Ru: C, 31.29 (31.29); H, 2.34 (2.09)
7	2067 s, 2030 s, 2011 ms, 2000 s, 1988 vs, 1951 w (sh)	C ₅₀ H ₃₆ O ₉ Os ₃ P ₂ Ru·1/2C ₆ H ₁₄ : C, 40.68 (40.84); H, 2.58 (2.76) ^[a]
8	2073 w, 2061 m, 2031 m, 2008 s, 1987 m, 1960 w, 1918 vw (br)	C ₃₄ H ₂₈ O ₉ Os ₃ P ₂ Ru·1/2CH ₂ Cl ₂ : C, 30.82 (30.79); H, 1.85 (2.11) ^[b]

[a] ¹H NMR spectroscopy confirmed the presence of hexane in the sample. [b] ¹H NMR spectroscopy confirmed the presence of dichloromethane in the sample.

reaction mixture was stirred and heated under reflux for 4 h. The solvent was removed under reduced pressure, and the residue obtained was redissolved in a minimum of dichloromethane and chromatographed on TLC plates with hexane/dichloromethane (3:2, v/v) as the mobile phase to afford unreacted **3a** ($R_f = 0.27$, yield = 10.1 mg) and **4a** ($R_f = 0.22$, yield = 10.0 mg, 50%). Similar ther-

molysis of **3b** (12.5 mg, 10 μ mol) afforded **4b** ($R_f = 0.57$, yield = 7.0 mg, 54%) and unreacted **3b** ($R_f = 0.51$, yield = 5.1 mg); and of **3c** (14.7 mg, 11 μ mol) afforded **4c** ($R_f = 0.31$, yield = 12.2 mg, 81%) and unreacted **3c** ($R_f = 0.26$, yield = 2.0 mg). For **3d** and **3e**, the infrared spectra and TLC analyses revealed only the presence of the starting clusters.

Table 5. NMR spectroscopic and MS data for all products.

Cluster	$^{31}\text{P}\{\text{H}\}$ NMR, δ	^1H NMR, δ	FAB-MS, m/z found (calculated for M^+)
2	77.40 (d, RuPOs, $^2J_{\text{PP}} = 116.4$ Hz) –22.34 (d, OsPOs)	7.64 (m, 5 H, Ph), 7.42 (s, 5 H, Ph), 5.97 (m, 1 H, CH ₂), 5.59 (m, 1 H, CH ₂)	1239 (1238)
3a	194.46 (d, PPh, $^2J_{\text{PP}} = 53.4$ Hz), –49.64 (d, PPh ₂)	7.93–6.85 (m, 25 H, Ph), 5.25 (m, 2 H, CH ₂), –17.43 (d, 1 H, OsHOs, $^2J_{\text{PH}} = 25.6$ Hz)	1411 (1410)
3b	190.86 (d, PPh, $^2J_{\text{PP}} = 53.5$ Hz), –46.88 (d, PPh ₂)	7.90–7.10 (m, 10 H, Ph), 5.79 (m, 1 H, CH ₂), 4.53 (m, 1 H, CH ₂), 2.55 (m, 2 H, CH ₂), 1.86 (s, 3 H, CH ₃), 1.06 (t, 3 H, CH ₃), –18.09 (d, 1 H, OsHOs, $^2J_{\text{PH}} = 26.2$ Hz)	1300 (1300)
3c	190.55 (d, PPh, $^2J_{\text{PP}} = 53.4$ Hz), –48.57 (d, PPh ₂)	7.92–7.49 (m, 15 H, Ph), 5.83 (m, 1 H, CH ₂), 5.95 (m, 1 H, CH ₂), 2.27 (s, 3 H, CH ₃), 2.07 (s, 9 H, <i>t</i> Bu), –18.03 (d, 1 H, OsHOs, $^2J_{\text{PH}} = 27.2$ Hz)	1329 (1328)
3d	196.28 (d, PPh, $^2J_{\text{PP}} = 49.6$ Hz), –45.82 (d, PPh ₂)	7.82–7.39 (m, 20 H, Ph), 5.44 (m, 1 H, CH ₂), 4.88 (m, 1 H, CH ₂), 1.27 (s, 1 H, CH), –17.74 (d, 1 H, OsHOs, $^2J_{\text{PH}} = 26.4$ Hz)	1335 (1334)
3e	203.52 (d, PPh, $^2J_{\text{PP}} = 53.4$ Hz), –47.32 (d, PPh ₂)	7.82–7.30 (m, 15 H, Ph), 5.51 (m, 1 H, CH ₂), 4.86 (m, 1 H, CH ₂), 1.73 (s, 1 H, CH), 1.26 (s, 9 H, <i>t</i> Bu), –18.02 (d, 1 H, OsHOs, $^2J_{\text{PH}} = 26.4$ Hz)	1314 (1314)
4a [major isomer]	196.92 (d, PPh, $^2J_{\text{PP}} = 93.5$ Hz), –33.94 (d, PPh ₂)	7.75–6.99 (m, 25 H, Ph), 4.02 (m, 2 H, CH ₂), –18.93 (ddd, 1 H, RuHOs, $^2J_{\text{PH}} = 9.9$ Hz, $^2J_{\text{PH}} = 8.9$ Hz, $^4J_{\text{HH}} = 3.3$ Hz)	1410 (1410)
[minor isomer]	135.84 (d, PPh, $^2J_{\text{PP}} = 87.7$ Hz), –32.92 (d, PPh ₂)	7.75–6.99 (m, 25 H, Ph), 4.02 (m, 2 H, CH ₂), –18.84 (ddd, 1 H, OsHOs, unresolved)	
4b [major isomer]	203.11 (d, PPh, $^2J_{\text{PP}} = 97.3$ Hz), –34.84 (d, PPh ₂)	7.75–6.91 (m, 15 H, Ph), 3.98 (m, 1 H, CH ₂), 3.85 (m, 1 H, CH ₂), 3.11 (d, 2 H, CH ₂), 2.96 (s, 3 H, CH ₃), 1.40 (t, 3 H, CH ₃), –19.50 (ddd, 1 H, RuHOs, $^2J_{\text{PH}} = 16.5$ Hz, $^2J_{\text{PH}} = 10.7$ Hz, $^4J_{\text{HH}} = 3.3$ Hz)	1300 (1300)
[minor isomer]	199.66 (d, PPh, $^2J_{\text{PP}} = 99.2$ Hz), –35.38 (d, PPh ₂)	7.75–6.91 (m, 15 H, Ph), 3.98–3.11 (m, 4 H, CH ₂), 2.96 (s, 3 H, CH ₃), 1.36 (t, 3 H, CH ₃), –19.45 (ddd, 1 H, OsHOs, unresolved)	
4c [major isomer]	209.36 (d, PPh, $^2J_{\text{PP}} = 99.2$ Hz), –35.54 (d, PPh ₂)	7.73–6.87 (m, 15 H, Ph), 3.82 (m, 2 H, CH ₂), 3.29 (s, 12 H, <i>t</i> Bu, CH ₃), –19.59 (ddd, 1 H, RuHOs, $^2J_{\text{PH}} = 15.3$ Hz, $^2J_{\text{PH}} = 10.3$ Hz, $^4J_{\text{HH}} = 3.3$ Hz)	1328 (1328)
[minor isomer I]	146.38 (d, PPh, $^2J_{\text{PP}} = 91.6$ Hz), –34.35 (d, PPh ₂)	7.60–6.87 (m, 15 H, Ph), 4.20 (m, 1 H, CH ₂), 3.85 (m, 1 H, CH ₂), 2.95 (s, 12 H, <i>t</i> Bu, CH ₃), –19.47 (ddd, 1 H, OsHOs, $^2J_{\text{PH}} = 14.0$ Hz, $^2J_{\text{PH}} = 8.3$ Hz, $^4J_{\text{HH}} = 2.5$ Hz)	
[minor isomer II]	216.21 (d, PPh, $^2J_{\text{PP}} = 91.6$ Hz), –35.80 (d, PPh ₂)	7.60–6.87 (m, 15 H, Ph), 4.37 (m, 1 H, CH ₂), 3.85 (m, 1 H, CH ₂), 3.32 (s, 12 H, <i>t</i> Bu, CH ₃), –19.21 (ddd, 1 H, OsHOs, $^2J_{\text{PH}} = 13.8$ Hz, $^2J_{\text{PH}} = 8.0$ Hz, $^4J_{\text{HH}} = 2.7$ Hz)	
5 [isomer I]	101.02 (d, PPh, $^2J_{\text{PP}} = 125.9$ Hz), –34.21 (d, PPh ₂)	7.70–7.32 (m, 15 H, Ph), 5.12 (m, 1 H, CH ₂), 4.71 (m, 1 H, CH ₂), 3.01 (d, 9 H, <i>t</i> Bu, $^2J_{\text{PH}} = 3.3$ Hz), 2.96 (m, 3 H, CH ₃), –15.54 (dd, 1 H, RuHOs, $^2J_{\text{PH}} = 17.3$ Hz, $^3J_{\text{PH}} = 8.3$ Hz)	1356 (1356)
[isomer II]	47.40 (d, PPh, $^2J_{\text{PP}} = 125.9$ Hz), –30.53 (d, PPh ₂)	7.70–7.32 (m, 15 H), 5.00 (m, 1 H, CH ₂), 4.36 (m, 1 H, CH ₂), 2.91 (m, 3 H, CH ₃), 2.85 (d, 9 H, <i>t</i> Bu, $^2J_{\text{PH}} = 3.3$ Hz), –15.02 (dd, 1 H, OsHOs, $^2J_{\text{PH}} = 12.4$ Hz, $^3J_{\text{PH}} = 9.1$ Hz)	
6 [major isomer]	152.56 (d, PPh, $^2J_{\text{PP}} = 53.4$ Hz), –45.81 (d, PPh ₂)	8.55 (s, 1 H, CHO), 7.67–7.59 (m, 15 H, Ph), 5.79 (m, 1 H, CH ₂), 4.92 (m, 1 H, CH ₂), 1.44 (s, 9 H, <i>t</i> Bu), –18.37 (d, 1 H, RuHOs, $^2J_{\text{PH}} = 23.6$ Hz)	1343 (1343)
[minor isomer]	198.70 (d, PPh, $^2J_{\text{PP}} = 49.6$ Hz), –51.79 (d, PPh ₂)	8.88 (s, 1 H, CHO), 7.90–7.83 (m, 15 H, Ph), 4.66 (m, 1 H, CH ₂), 4.21 (m, 1 H, CH ₂), 1.33 (s, 9 H, <i>t</i> Bu), –18.20 (d, 1 H, OsHOs, $^2J_{\text{PH}} = 27.2$ Hz)	
7	3.86 (d, PPh ₂ , $^2J_{\text{PP}} = 45.8$ Hz), –6.34 (d, PPh ₂)	7.55–6.89 (m, 30 H, Ph), 6.58 (s, 1 H, PhC=CHCCHPh), 5.78 (m, 1 H, PhC=CHCCHPh), 4.66 (m, 1 H, CH ₂), 3.79 (m, 1 H, CH ₂), –13.12 (dt, 1 H, RuHOs, $^2J_{\text{PH}} = 16.5$, $^3J_{\text{PH}} = 5.0$, $^2J_{\text{HH}} = 5.0$ Hz), –17.62 (dt, 1 H, OsHOs, $^2J_{\text{PH}} = 11.5$, $^2J_{\text{PH}} = 11.5$, $^2J_{\text{HH}} = 5.0$ Hz)	1514 (1514)
8 [major isomer]	–21.40 (d, PPh, $^2J_{\text{PP}} = 36.3$ Hz), –1.82 (d, PPh ₂)	7.62–7.49 (m, 10 H, Ph), 7.22–7.11 (m, 5 H, Ph), 5.40 (m, 2 H, CH ₂), 2.24 (m, 1 H, CH), 1.22 (s, 9 H, <i>t</i> Bu), –20.23 (ddd, 1 H, OsHOs, $^2J_{\text{PH}} = 19.0$ Hz, $^2J_{\text{PH}} = 12.8$ Hz, $^4J_{\text{HH}} = 5.8$ Hz)	1344 (1342)
[minor isomer]	–20.52 (d, PPh, $^2J_{\text{PP}} = 40.0$ Hz), 2.83 (d, PPh ₂)	7.75–7.65 (m, 10 H, Ph), 7.19–7.12 (m, 5 H, Ph), 5.51 (m, 2 H, CH ₂), 2.31 (m, 1 H, CH), 1.25 (s, 9 H, <i>t</i> Bu), –20.20 (ddd, 1 H, OsHOs, $^2J_{\text{PH}} = 18.3$ Hz, $^2J_{\text{PH}} = 14.0$ Hz, $^4J_{\text{HH}} = 5.0$ Hz)	

4.6. Thermolysis of 5: To a Schlenk tube containing **5** (10.3 mg, 0.008 mmol) was added hexane (30 mL), and the reaction mixture was stirred and heated under reflux for 4 h. Subsequent treatment as above afforded unreacted **5** (3.5 mg), **4c** (2.5 mg, 23%), and **3c** (3.7 mg, 34%).

4.7. Reaction of 1 with 4,4-Dimethyl-2-pentyne in Air: To a 100-mL two-necked, round-bottomed flask containing **1** (12.1 mg, 0.009 mmol) and hexane (30 mL) was added *t*BuCCCH₃ (0.1 mL). Air was bubbled into the mixture by means of a compressor pump and the reaction mixture was stirred and heated under reflux for 6 h. Subsequent treatment as above afforded **5** (1.8 mg, 15%), **4c** (2.9 mg, 24%), **3c** (3.5 mg, 29%) and **6** (1.8 mg, 15%).

4.8. Thermolysis of 3c, 4c, or 5 in Air: To a 100-mL two-necked, round-bottomed flask containing **3c** (7.1 mg, 0.005 mmol), **4c** (5.2 mg, 0.004 mmol), or **5** (8.4 mg, 0.006 mmol) was added hexane (30 mL). Air was bubbled into the mixture by means of a compressor pump and the reaction mixture was stirred and heated under reflux for 6 h. Subsequent treatment as above revealed the presence of all three clusters for the thermolysis of **5**. Clusters **3c** and **4c** were obtained from the reaction of **3c**, while only the unreacted starting cluster was observed when **4c** was heated.

4.9. Reaction of 1 with Phenylacetylene: To a Schlenk tube containing **1** (9.9 mg, 0.007 mmol) and hexane (30 mL) was added phenylacetylene (0.1 mL), and the reaction mixture was stirred and heated under reflux for 12 h. Subsequent treatment as above afforded triphenylbenzene (1.0 mg), **3d** (3.3 mg, 36%) and **7** (4.9 mg, 46%).

4.10. Thermolysis of 8: To a Schlenk tube containing **8** (8.4 mg, 0.006 mmol) was added hexane (30 mL), and the reaction mixture was stirred and heated under reflux for 4 h. Subsequent treatment as above afforded unreacted **8** (3.8 mg) and **3e** (4.3 mg, 54%).

4.11. Cyclotrimerization Reactions of Phenylacetylene: In a typical reaction, the cluster **3d** and PhCCH were placed in a Carius tube containing hexane (10 mL), degassed by three freeze-pump-thaw cycles, and heated.

4.12. Reaction of 3d with Diphenylacetylene and *tert*-Butylacetylene: To a Schlenk tube containing **3d** (5.2 mg, 0.004 mmol) and hexane (30 mL) was added PhCCPh (6.1 mg, 0.030 mmol) or *t*BuCCCH (0.1 mL), and the reaction mixture was stirred and heated under reflux for 12 h. Subsequent treatment as above revealed the presence of unreacted **3d** only.

4.13 X-ray Crystal Structure Determinations

Crystals were mounted on quartz fibers. X-ray data were collected with a Bruker AXS APEX system, by using Mo-*K*_α radiation, with the SMART suite of programs.^[29] Data were processed and corrected for Lorentz and polarization effects with SAINT,^[30] and for absorption effects with SADABS.^[31] Structural solution and refinement were carried out with the SHELXTL suite of programs.^[32] Crystal and refinement data are summarized in Table 6, Table 7, and Table 8.

The structures were solved by direct methods to locate the heavy atoms, followed by difference maps for the light, non-hydrogen atoms. The hydrides were generally placed by potential energy calculations with the program XHYDEX,^[19] given fixed isotropic thermal parameters, and refined riding on an osmium atom to which they are attached. Organic hydrogen atoms were generally placed in calculated positions and refined with a riding model. All non-hydrogen atoms were generally given anisotropic displacement parameters in the final model.

Cluster **2** sits across a C₂ symmetry axis, which passes through the methylene carbon of the dppm ligand and the midpoint of the

Table 6. Crystal data for **2**, **3a–c**.

Compound	2	3a	3b	3c
Formula	C ₂₅ H ₁₂ O ₁₂ Os ₃ P ₂ Ru	C ₄₂ H ₂₈ O ₉ Os ₃ P ₂ Ru·1/2CH ₂ Cl ₂	C ₃₃ H ₂₆ O ₉ Os ₃ P ₂ Ru	C ₃₅ H ₃₀ O ₉ Os ₃ P ₂ Ru·1/2C ₆ H ₁₄
Formula weight	1237.96	1452.72	1300.15	1371.29
Temperature [K]	193(2)	223(2)	223(2)	223(2)
Crystal system	Monoclinic	Triclinic	Tetragonal	Triclinic
Space group	C2/c	P $\bar{1}$	I42d	P $\bar{1}$
Unit cell dimensions				
<i>a</i> [Å]	16.119(3)	9.1091(2)	31.5814(6)	9.0388(4)
<i>b</i> [Å]	9.2446(17)	13.6379(3)	31.5814(6)	12.2045(5)
<i>c</i> [Å]	21.004(4)	17.8813(5)	15.6854(6)	18.9635(8)
<i>α</i> [°]	90	96.0940(10)	90	74.2140(10)
<i>β</i> [°]	98.507(9)	99.4940(10)	90	81.7690(10)
<i>γ</i> [°]	90	97.656(2)	90	78.3480(10)
Volume [Å ³]	3095.3(10)	2152.68(9)	15644.4(7)	1962.90(14)
<i>Z</i>	4	2	16	2
<i>ρ</i> _c [g cm ⁻³]	2.656	2.241	2.208	2.320
<i>μ</i> (Mo- <i>K</i> _α) [mm ⁻¹]	12.916	9.359	10.222	10.190
<i>F</i> (000)	2240	1350	9568	1278
Crystal size [mm ³]	0.34 × 0.28 × 0.18	0.10 × 0.20 × 0.26	0.30 × 0.26 × 0.20	0.34 × 0.16 × 0.10
<i>θ</i> range [°]	2.55 to 29.98	2.03 to 28.28	2.04 to 26.37	2.24 to 28.28
Reflections collected	12731	19531	58395	27491
Independent reflections (<i>R</i> _{int})	4308 [<i>R</i> (int) = 0.0402]	10590 (0.0395)	8009 (0.0432)	9695 (0.0441)
Completeness%, (to <i>θ</i> , deg)	95.7 (29.98)	99.2 (28.28)	99.9 (26.37)	99.5 (28.28)
Transmission range	0.2046 and 0.0965	0.298003–0.170804	0.2343–0.1494	0.4289–0.1292
Data/restraints/parameters	4308/0/195	10590/0/544	8009/0/436	9695/1/468
Goodness-of-fit on <i>F</i> ²	1.066	1.011	1.162	1.051
Final <i>R</i> indices [<i>I</i> > 2σ(<i>I</i>)]	<i>R</i> ₁ = 0.0313, <i>wR</i> ₂ = 0.0734	<i>R</i> ₁ = 0.0410, <i>wR</i> ₂ = 0.1037	<i>R</i> ₁ = 0.0298, <i>wR</i> ₂ = 0.0857	<i>R</i> ₁ = 0.0392, <i>wR</i> ₂ = 0.0930
<i>R</i> indices (all data)	<i>R</i> ₁ = 0.0362, <i>wR</i> ₂ = 0.0769	<i>R</i> ₁ = 0.0508, <i>wR</i> ₂ = 0.1073	<i>R</i> ₁ = 0.0323, <i>wR</i> ₂ = 0.0868	<i>R</i> ₁ = 0.0485, <i>wR</i> ₂ = 0.0970
Largest diff. peak and hole [e Å ⁻³]	1.271 and -2.538	2.405 and -1.342	1.754 and -0.747	2.953 and -1.566

Table 7. Crystal data for **3d–e** and **4a–b**.

Compound	3d	3e	4a	4b
Formula	C ₃₆ H ₂₄ O ₉ Os ₃ P ₂ Ru	C ₃₄ H ₂₈ O ₉ Os ₃ P ₂ Ru	C ₄₂ H ₂₈ O ₉ Os ₃ P ₂ Ru	C ₃₃ H ₂₆ O ₉ Os ₃ P ₂ Ru
Formula weight	1334.16	1314.17	1410.25	1300.15
Temperature [K]	223(2)	193(2)	223(2)	223(2)
Crystal system	Triclinic	Triclinic	Monoclinic	Monoclinic
Space group	<i>P</i> $\bar{1}$	<i>P</i> $\bar{1}$	<i>Cc</i>	<i>P</i> ₂ / <i>c</i>
Unit cell dimensions				
<i>a</i> [Å]	8.7605(2)	8.8328(4)	11.5027(11)	9.0451(8)
<i>b</i> [Å]	12.5261(3)	12.3241(5)	21.5495(19)	26.643(2)
<i>c</i> [Å]	17.1932(3)	16.9444(7)	33.708(3)	14.7236(12)
α [°]	103.2880(10)	96.4610(10)	90	90
β [°]	96.6360(10)	92.4220(10)	92.971(4)	102.134(2)
γ [°]	98.3850(10)	100.2260(10)	90	90
Volume [Å ³]	1794.65(7)	1800.02(13)	8344.3(14)	3468.9(5)
<i>Z</i>	2	2	8	4
ρ_c [g cm ^{−3}]	2.469	2.425	2.245	2.489
μ (Mo- <i>K</i> α) [mm ^{−1}]	11.142	11.107	9.592	11.525
<i>F</i> (000)	1228	1212	5232	2392
Crystal size [mm ³]	0.36 × 0.28 × 0.22	0.14 × 0.08 × 0.02	0.12 × 0.08 × 0.04	0.22 × 0.20 × 0.02
θ range [°]	2.33 to 28.28	2.57 to 29.49	2.01 to 24.71	2.08 to 26.37
Reflections collected	16218	21674	28930	50407
Independent reflections (<i>R</i> _{int})	8827 (0.0283)	8932 (0.0651)	10896 (0.0797)	7096 (0.0825)
Completeness%, (to θ , deg)	99.0 (28.28)	99.3 (26.37)	99.8 (24.71)	99.9 (26.37)
Transmission range	0.1930–0.1080	0.6659–0.4714	0.7002–0.3923	0.8022–0.1859
Data/restraints/parameters	8827/0/468	8932/0/449	10896/8/608	7096/0/439
Goodness-of-fit on <i>F</i> ²	1.066	1.074	0.964	1.020
Final <i>R</i> indices [<i>I</i> > 2 σ (<i>I</i>)]	<i>R</i> ₁ = 0.0311, <i>wR</i> ₂ = 0.0737	<i>R</i> ₁ = 0.0472, <i>wR</i> ₂ = 0.0925	<i>R</i> ₁ = 0.0531, <i>wR</i> ₂ = 0.1006	<i>R</i> ₁ = 0.0404, <i>wR</i> ₂ = 0.0996
<i>R</i> indices (all data)	<i>R</i> ₁ = 0.0366, <i>wR</i> ₂ = 0.0757	<i>R</i> ₁ = 0.0652, <i>wR</i> ₂ = 0.1035	<i>R</i> ₁ = 0.0950, <i>wR</i> ₂ = 0.1211	<i>R</i> ₁ = 0.0514, <i>wR</i> ₂ = 0.1054
Largest diff. peak and hole [e Å ^{−3}]	2.201 and −1.347	1.947 and −1.660	1.921 and −2.259	3.143 and −1.816

Table 8. Crystal data for **5–8**.

Compound	5	6	7	8
Formula	C ₃₆ H ₃₀ O ₁₀ Os ₃ P ₂ Ru	C ₃₅ H ₂₈ O ₁₀ Os ₃ P ₂ Ru·1/2CH ₂ Cl ₂	C ₅₀ H ₃₆ O ₉ Os ₃ P ₂ Ru	C ₃₅ H ₂₈ O ₁₀ Os ₃ P ₂ Ru·CH ₂ Cl ₂
Formula weight	1356.21	1384.65	1514.40	1427.11
Temperature [K]	223(2)	223(2)	223(2)	193(2)
Crystal system	Triclinic	Monoclinic	Monoclinic	Triclinic
Space group	<i>P</i> $\bar{1}$	<i>C</i> 2/ <i>c</i>	<i>P</i> ₂ / <i>c</i>	<i>P</i> $\bar{1}$
Unit cell dimensions				
<i>a</i> [Å]	10.2517(6)	34.9452(14)	18.7787(6)	10.8185(4)
<i>b</i> [Å]	10.7899(6)	12.7259(5)	12.0922(4)	12.4511(5)
<i>c</i> [Å]	19.2191(10)	24.3102(9)	22.0276(7)	15.3985(6)
α [°]	93.9060(10)	90	90	88.2510(10)
β [°]	96.1960(10)	129.3270(10)	111.0870(10)	75.3930(10)
γ [°]	113.9100(10)	90	90	86.3140(10)
Volume [Å ³]	1917.43(18)	8362.7(6)	4667.0(3)	2002.80(13)
<i>Z</i>	2	8	4	2
ρ_c [g cm ^{−3}]	2.349	2.200	2.155	2.366
μ (Mo- <i>K</i> α) [mm ^{−1}]	10.432	9.632	8.584	10.123
<i>F</i> (000)	1256	5128	2840	1324
Crystal size [mm ³]	0.10 × 0.12 × 0.24	0.38 × 0.27 × 0.10	0.32 × 0.18 × 0.05	0.38 × 0.26 × 0.08
θ range [°]	2.15 to 26.37	2.17 to 24.71	2.05 to 29.48	2.08 to 30.03
Reflections collected	28297	62952	65040	29989
Independent reflections (<i>R</i> _{int})	7791 (0.0350)	7119 (0.0432)	12163 (0.0542)	11306 (0.0324)
Completeness%, (to θ , deg)	99.4 (26.37)	99.9 (24.71)	93.7 (29.48)	96.4 (30.03)
Transmission range	0.4218–0.1886	0.4459–0.1208	0.6735–0.1698	0.4981–0.1137
Data/restraints/parameters	7791/2/476	7119/18/490	12163/0/586	11306/0/497
Goodness-of-fit on <i>F</i> ²	1.037	1.097	1.308	1.043
Final <i>R</i> indices [<i>I</i> > 2 σ (<i>I</i>)]	<i>R</i> ₁ = 0.0319, <i>wR</i> ₂ = 0.0796	<i>R</i> ₁ = 0.0528, <i>wR</i> ₂ = 0.1070	<i>R</i> ₁ = 0.0533, <i>wR</i> ₂ = 0.0991	<i>R</i> ₁ = 0.0274, <i>wR</i> ₂ = 0.0716
<i>R</i> indices (all data)	<i>R</i> ₁ = 0.0369, <i>wR</i> ₂ = 0.0822	<i>R</i> ₁ = 0.0364, <i>wR</i> ₂ = 0.0847	<i>R</i> ₁ = 0.0590, <i>wR</i> ₂ = 0.1011	<i>R</i> ₁ = 0.0310, <i>wR</i> ₂ = 0.0731
Largest diff. peak and hole [e Å ^{−3}]	2.728 and −1.418	1.851 and −1.000	2.368 and −1.375	2.552 and −1.897

hinge metal–metal bond. Cluster **3b** was refined as a racemic twin. There were two molecules in the asymmetric unit for **4a**. Disorder of the heavy atom positions were found for **2**, **3e**, **4a**, **4b**, **5**, **6**, and **8**. Solvent molecules were found in the crystals of **3a** (half molecule of CH₂Cl₂), **3c** (half molecule of hexane), and **6** (half molecule of CH₂Cl₂).

CCDC-628206–CCDC-628217 contain the supplementary crystallographic data for this paper. These data can be obtained free of charge from The Cambridge Crystallographic Data Centre via www.ccdc.cam.ac.uk/data_request/cif.

Supporting Information (see footnote on the first page of this article): Details on the treatment of disorder, metal hydride placement and refinement, and of solvent molecules in the X-ray crystallographic studies; ³¹P{¹H}-¹H HMBC spectra for **4c**, **5**, and **7**; ³¹P{¹H}-³¹P{¹H} COSY spectrum for **4c**; the isomerization of **3c** and **4c** (percentages against time, as obtained from ¹H NMR spectra); cyclotrimerization reactions of **3d** with phenylacetylene.

Acknowledgments

This work was supported by the National University of Singapore (Research Grant No. R143-000-267-112) and one of us (Y. L. K. T.) thanks the University for a Research Scholarship.

- [1] a) B. Fontal, M. Reyes, T. Suárez, F. Bellandi, J. C. Diaz, *J. Mol. Catal. A* **1999**, *149*, 75; b) B. Fontal, M. Reyes, T. Suárez, F. Bellandi, J. C. Diaz, *J. Mol. Catal. A* **1999**, *149*, 87; c) C. Bergounhou, J. J. Bonnet, P. Fompeyrine, G. Lavigne, N. Logun, F. Mansilla, *Organometallics* **1986**, *5*, 60; d) C. Bergounhou, J. J. Bonnet, P. Fompeyrine, G. Commenges, *J. Mol. Catal.* **1988**, *48*, 285; e) U. Matteoli, V. Baghetto, A. Scrivanti, *J. Mol. Catal. A* **1996**, *109*, 45; f) V. Moberg, P. Homanen, S. Selva, R. Persson, M. Haukka, T. A. Pakkanen, M. Monari, E. Nordlander, *Dalton Trans.* **2006**, 279.
- [2] a) L. Pereira, W. K. Leong, S. Y. Wong, *J. Organomet. Chem.* **2000**, *609*, 104; b) L. J. Pereira, K. S. Chan, W. K. Leong, *J. Organomet. Chem.* **2005**, *690*, 1033; c) L. J. Pereira, W. K. Leong, *J. Organomet. Chem.* **2006**, *691*, 1941; d) L. J. Pereira, W. K. Leong, *J. Organomet. Chem.* **2006**, *691*, 2448; e) L. J. Pereira, W. K. Leong, *Polyhedron* **2006**, *25*, 2392; f) Y. L. K. Tan, W. K. Leong, *J. Organomet. Chem.* **2006**, *691*, 2048; g) Y. L. K. Tan, C. W. A. Koh, T. B. Lim, W. K. Leong, *J. Cluster Sci.* **2006**, *17*, 509; h) Y. L. K. Tan, W. K. Leong, *J. Organomet. Chem.* **2007**, *692*, 768.
- [3] Y. L. K. Tan, W. K. Leong, *J. Organomet. Chem.* in press.
- [4] a) G.-Y. Kiel, J. Takats, *Organometallics* **1989**, *8*, 839; b) K. A. Buntam, D. H. Farrar, A. J. Poë, A. J. Lough, *Organometallics* **2000**, *19*, 3674.
- [5] N. E. Leadbeater, J. Lewis, P. R. Raithby, A. J. Edwards, *J. Organomet. Chem.* **1997**, *545–546*, 567.
- [6] a) J. A. Clucas, M. M. Harding, A. K. Smith, *J. Chem. Soc., Chem. Commun.* **1985**, 1280; b) S. M. T. Abedin, K. I. Hardcastle, S. E. Kabir, K. M. A. Malik, M. A. Mottalib, E. Rosenberg, M. J. Abedin, *Organometallics* **2000**, *19*, 5623.
- [7] R. C. Pomeroy in *Comprehensive Organometallic Chemistry II* (Eds.: G. Wilkinson, F. G. A. Stone, E. W. Abel), Pergamon, Oxford, New York, **1995**, vol. 7, ch. 15.
- [8] M. I. Bruce, E. Horn, O. bin Shawkataly, M. R. Snow, E. R. T. Tiekink, M. L. Williams, *J. Organomet. Chem.* **1986**, *316*, 187.
- [9] A. J. Carty, S. A. MacLaughlin, D. Nuciurone in *Phosphorus-31 NMR Spectroscopy in Stereochemical Analysis: Organic Compounds and Metal Complexes* (Eds.: J. G. Verkade; L. D. Quinn), VCH, New York, **1987**.
- [10] a) G. Hogarth, J. A. Phillips, F. Van Gastel, N. J. Taylor, T. B. Marder, A. J. Carty, *J. Chem. Soc., Chem. Commun.* **1988**, 1570; b) G. Hogarth, N. Hadj-Bagheri, N. J. Taylor, A. J. Carty, *J. Chem. Soc., Chem. Commun.* **1990**, 1352; c) L. M. Bullock, J. S. Field, R. J. Haines, E. Minshall, M. H. Moore, F. Mulla, D. N. Smit, L. M. Steer, *J. Organomet. Chem.* **1990**, *381*, 429; d) A. M. Arif, T. Bright, D. E. Heaton, R. A. Jones, C. M. Nunn, *Polyhedron* **1990**, *9*, 1573; e) V. Patel, A. Cherkas, D. Nucciarone, N. J. Taylor, A. J. Carty, *Organometallics* **1985**, *4*, 1793.
- [11] a) A. A. Koridze, *Russ. Chem. Bull.* **2000**, *49*, 1135; b) S. Deabate, R. Giordano, E. Sappa, *J. Cluster Sci.* **1997**, *8*, 407; c) E. Sappa, A. Tiripicchio, A. J. Carty, G. E. Toogood, *Prog. Inorg. Chem.* **1987**, *35*, 437; d) P. R. Raithby, M. J. Rosales, *Adv. Inorg. Chem. Radiochem.* **1985**, *29*, 169; e) E. Sappa, A. Tiripicchio, P. Braunstein, *Chem. Rev.* **1983**, *83*, 203.
- [12] a) V. Ferrand, G. Süss-Fink, A. Neels, H. Stoeckli-Evans, *J. Chem. Soc., Dalton Trans.* **1998**, 3825; b) V. Ferrand, G. Süss-Fink, A. Neels, H. Stoeckli-Evans, *Eur. J. Inorg. Chem.* **1999**, 853.
- [13] M. B. Smith, J. March, *March's Advanced Organic Chemistry*, 5th ed., Wiley, New York, **2001**, p. 20.
- [14] a) P. Srinivasan, W. K. Leong, *Eur. J. Inorg. Chem.* **2006**, 464; b) G. Wilkinson, F. G. A. Stone, E. W. Abel (Eds.), *Comprehensive Organometallic Chemistry II*, Pergamon, Oxford-New York, **1995**; c) L. F. Dahl, D. L. Smith, *J. Am. Chem. Soc.* **1962**, *84*, 2450; d) R. J. Haines, N. D. C. T. Steen, M. Laing, P. Somerville, *J. Organomet. Chem.* **1980**, *198*, C72 and references cited therein.
- [15] a) M. R. Churchill, R. A. Lashewycz, *Inorg. Chem.* **1978**, *17*, 1950; b) R. D. Adams, N. M. Golembeski, J. P. Selegue, *J. Am. Chem. Soc.* **1981**, *103*, 546.
- [16] E. Sappa, A. Tiripicchio, P. Braunstein, *Coord. Chem. Rev.* **1985**, *65*, 219.
- [17] a) A. J. Deeming, M. Underhill, *J. Chem. Soc., Dalton Trans.* **1974**, 1415; b) A. J. Deeming, *J. Organomet. Chem.* **1978**, *150*, 123; c) A. J. Deeming, I. P. Rothwell, M. B. Hursthouse, J. D. Backer-Dirks, *J. Chem. Soc., Dalton Trans.* **1981**, 1879.
- [18] T. Takao, S. Kakuta, R. Tenjimbayashi, T. Takemori, E. Murotani, H. Suzuki, *Organometallics* **2004**, *23*, 6090.
- [19] A. G. Orpen, *XYDEX*, School of Chemistry, University of Bristol, UK, **1997**.
- [20] a) A. J. Deeming, *J. Mol. Catal.* **1983**, *21*, 25; b) A. J. Deeming, P. J. Manning, I. P. Rothwell, M. B. Hursthouse, N. P. C. Walker, *J. Chem. Soc., Dalton Trans.* **1984**, 2039; c) E. Boyar, A. J. Deeming, A. J. Arce, Y. De Sanctis, *J. Organomet. Chem.* **1984**, *276*, C45; d) A. J. Arce, Y. De Sanctis, A. J. Deeming, *J. Organomet. Chem.* **1985**, *295*, 365; e) A. J. Arce, Y. De Sanctis, A. J. Deeming, *Polyhedron* **1988**, *7*, 979.
- [21] a) S. Aime, L. Milone, D. Osella, M. Valle, *J. Chem. Res. (S)* **1978**, 77; b) S. Aime, D. Osella, *Organomet. Synth.* **1988**, *4*, 253; c) M. I. Bruce, A. C. Meier, B. W. Skelton, A. H. White, N. N. Zaitseva, *Aust. J. Chem.* **2001**, *54*, 319.
- [22] a) G. Gervasio, E. Sappa, A. M. M. Lanfredi, A. Tiripicchio, *Inorg. Chim. Acta* **1983**, *68*, 171; b) V. Ferrand, C. Gambs, N. Derrien, C. Bolm, H. Stoeckli-Evans, G. Süss-Fink, *J. Organomet. Chem.* **1997**, *549*, 275; c) L. J. Farrugia, N. Macdonald, R. D. Peacock, *Polyhedron* **1998**, *17*, 2877.
- [23] a) O. Gambino, E. Sappa, A. M. M. Lanfredi, A. Tiripicchio, *Inorg. Chim. Acta* **1979**, *36*, 189; b) R. D. Adams, J. E. Babin, M. Tasi, J.-G. Wang, *Organometallics* **1988**, *7*, 755.
- [24] a) J. F. Corrigan, S. Doherty, N. J. Tylor, A. J. Carty, *Organometallics* **1993**, *12*, 1365; b) M. I. Bruce, J. R. Hinchcliff, P. A. Humphrey, R. J. Surynt, B. W. Skelton, A. H. White, *J. Organomet. Chem.* **1998**, *552*, 109; c) M. I. Bruce, S. I. Pyke, N. N. Zaitseva, B. W. Skelton, A. H. White, *Helv. Chim. Acta* **2001**, *84*, 3197.
- [25] a) K. Lonsdale, *Nature* **1934**, *133*, 67; b) K. S. Krishnan, S. Banerjee, *Nature* **1934**, *133*, 497; c) G. Booth, J. M. Rowe, *Chem. Ind.* **1960**, 661.
- [26] See for example: a) M. S. Sigman, A. W. Fatland, B. E. Eaton, *J. Am. Chem. Soc.* **1998**, *120*, 5130; b) Y. Sato, K. Ohashi, M. Mori, *Tetrahedron Lett.* **1999**, *40*, 5231; c) N. Mori, S. Ikeda, K. Odashima, *Chem. Commun.* **2001**, 181.

- [27] a) W. Hübel, C. Hoogzand, *Chem. Ber.* **1960**, *93*, 103; b) M. Valle, G. Cetini, O. Gambino, E. Sappa, *Atti Accad. Sci. Torino* **1969**, *105*, 913; c) G. A. Vaglio, O. Gambino, R. P. Ferrari, G. Cetini, *Inorg. Chim. Acta* **1973**, *7*, 193; d) C. C. Yin, A. J. Deeming, *J. Organomet. Chem.* **1978**, *144*, 351; e) C. Y. Ren, W. C. Cheng, W. C. Chan, C. H. Yeung, C. P. Lau, *J. Mol. Catal.* **1990**, *59*, L1; f) W. Baidossi, N. Goren, J. Blum, H. Schumann, H. Hemling, *J. Mol. Catal.* **1993**, *85*, 153; g) A. J. Edwards, N. E. Leadbeater, J. Lewis, P. R. Raithby, *J. Chem. Soc., Dalton Trans.* **1995**, 3985; h) T. Sugihara, A. Wakabayashi, Y. Nagai, H. Takao, H. Imagawa, M. Nishizawa, *Chem. Commun.* **2002**, 576; i) M. Deng, W. K. Leong, *Organometallics* **2002**, *21*, 1221.
- [28] H. D. Kaesz, *Inorg. Synth.* **1990**, *28*, 238.
- [29] *SMART* version 5.628, Bruker AXS Inc. Madison, Wisconsin, USA, **2001**.
- [30] *SAINT+* version 6.22a, Bruker AXS Inc. Madison, Wisconsin, USA, **2001**.
- [31] G. M. Sheldrick, *SADABS*, **1996**.
- [32] *SHELXTL* version 5.1, Bruker AXS Inc., Madison, Wisconsin, USA, **1997**.

Received: November 27, 2006
Published Online: March 6, 2007